Structural Characterization of PNA–DNA Duplexes by NMR. Evidence for DNA in a B-like Conformation†

Mikael Leijon,‡ Astrid Gräslund,‡ Peter E. Nielsen,§ Ole Buchardt,∥ Bengt Nordén,⊥ Søren M. Kristensen,∥ and Magdalena Eriksson*,§,∥

Department of Biophysics, Arrhenius Laboratory, Stockholm University, S-106 91 Stockholm, Sweden, Centre for Biomolecular Recognition, IMBG, Laboratory B, The Panum Institute, Blegdamsvej 3C, DK-2200 Copenhagen N, Denmark, Department of Chemistry, The H. C. Ørsted Institute, University of Copenhagen, Universitetsparken 5, DK-2100 Copenhagen Ø, Denmark, and Department of Physical Chemistry, Chalmers University of Technology, S-412 96 Göteborg, Sweden

Received May 9, 1994; Revised Manuscript Received June 22, 1994®

ABSTRACT: The nucleic acid analogues PNA (peptide nucleic acids) hybridize with DNA of complementary sequence. The solution structures of two PNA–DNA duplexes, H-(GCTATGTC)-NH_2-d(GACATAGC) and H-(GTAGATCACT)-NH_2-d(AGTGATCTAC), have been studied by ^1H NMR. It was found that the PNA–DNA hybrids are base paired by hydrogen bonds, most likely of the Watson–Crick type. From two-dimensional NOESY and COSY results it is concluded that the DNA strand in the PNA–DNA complex adopts a B-like structure with the deoxyribose sugars in the C2′-*endo* conformation.

Peptide nucleic acid (PNA) is a DNA analogue in which the natural phosphate–deoxyribose backbone has been replaced by a pseudo peptide chain consisting of *N*-(2-aminoethyl)-glycine units (Chart 1) (Nielsen et al., 1991). PNA is homomorphous to DNA, with the same number of bonds in each unit along the backbone as well as in the linker to which any of the four nucleobases can be attached. The achiral and electrostatically neutral PNA molecule is capable of recognizing its complementary sequence in DNA and RNA (Egholm et al., 1993) as well as in PNA (Wittung et al., 1994), according to the Watson–Crick base-pairing rules (Egholm et al., 1993). PNA sequences rich in pyrimidines bind to complementary DNA oligonucleotides forming $(PNA)_2DNA$ triplexes (Egholm et al., 1992; Kim et al., 1993), and to double-stranded DNA by strand invasion, displacing the noncomplementary strand and thereby creating a P-loop complex (Nielsen et al., 1991, 1994; Cherny, et al., 1992). PNA–DNA hybrid duplexes are considerably more stable than the corresponding DNA–DNA duplexes, which is believed mainly to be due to the lack of electrostatic repulsion between the two strands (Egholm et al., 1993). Moreover, duplexes can be formed with both parallel and antiparallel orientation of the PNA and DNA strands; however, the latter is more stable (Egholm et al., 1993). Various lines of experiments have shown that PNA has interesting potentials as antisense (Hanvey et al., 1992; Demidov et al., 1994) and antigene drugs (Nielsen et al., 1992, 1993; Hanvey et al., 1992) and as biomolecular and diagnostic tools (Nielsen et al., 1993; Demidov et al., 1993; Ørum et al., 1993).

The structural properties of the PNA–DNA complexes are of high interest. However, the information about the structural details has so far been very limited. Flow linear dichroism and circular dichroism (CD) spectroscopy experiments on $(PNA)_2DNA$ triplexes have shown that the base planes are nearly perpendicularly oriented relative to the molecular long axis and that the structure is relatively inflexible (Kim et al., 1993). Furthermore, CD studies of antiparallel duplexes between PNA and DNA or RNA have indicated that these adopt right-handed helical structures, with base-pair stacking similar to A- or B-form DNA (Egholm et al., 1993). Here we present the first NMR results on the structure of the antiparallel PNA–DNA duplex. The data show that the PNA–DNA duplexes are bound via hydrogen bonds, most likely of the Watson–Crick type, and that the DNA strand is in a B-like conformation.

Chart 1

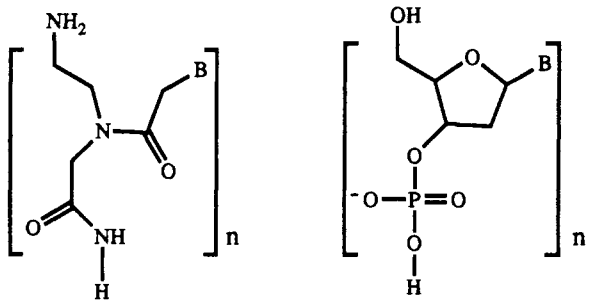

MATERIALS AND METHODS

The PNA strands were synthesized as previously described (Egholm et al., 1992). DNA oligonucleotides, purified by HPLC, were purchased from Symbicom AB, Umeå, Sweden, and were used without further purification. The PNA–DNA 8-mer duplex was kept in a 10 mM phosphate aqueous buffer solution, pH 6.5, containing 100 mM NaCl and 0.1 mM EDTA. The PNA–DNA 10-mer duplex was dissolved either in D_2O containing 5 mM phosphate buffer, pH 7.0, or in H_2O containing 50 mM phosphate buffer, pH 7.0. The DNA–DNA 10-mer duplex was studied at 1.8 mM duplex concentration in H_2O solution containing 10 mM phosphate buffer, pH 7.0, and 100 mM NaCl. Sample concentrations were determined by UV absorption measurements using molar extinction coefficients of 185 500 M^{-1} cm^{-1} for the 8-mer

† This study was supported by the Swedish Natural Science Research Council and the Magn. Bergwall Foundation.

* Author to whom correspondence should be addressed at the Panum Institute.

‡ Stockholm University.

§ The Panum Institute.

∥ University of Copenhagen.

⊥ Chalmers University of Technology.

® Abstract published in *Advance ACS Abstracts,* August 1, 1994.

0006-2960/94/0433-9820$04.50/0

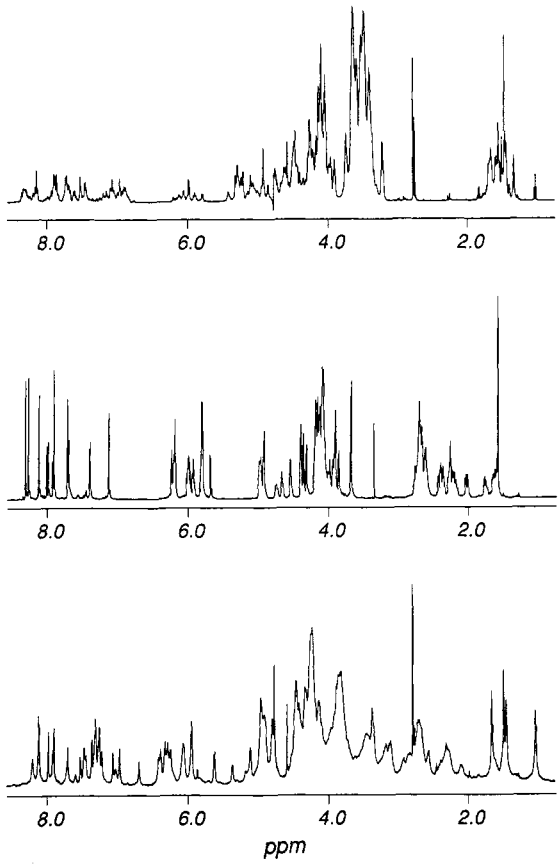

FIGURE 1: ^{1}H NMR spectra of H-GCTATGTC-NH_2 (a, top), d(GACATAGC) (b, middle), and the d(GACATAGC)·H-GC-TATGTC-NH_2 duplex at a 1:1 ratio (c, bottom), in D_2O solution at 24 °C.

PNA–DNA duplex and 210 000 M^{-1} cm^{-1} for the 10-mer PNA–DNA and DNA–DNA duplexes. NOESY data recorded in D_2O were collected in the TPPI mode (Marion & Wüthrich, 1983) on a Bruker AM-500 NMR spectrometer. The NOESY experiments on the 10-mer and the DQF-COSY experiment on the 8-mer were conducted with the hypercomplex method (States et al., 1982) on a Varian Unity 500 spectrometer. For the NOESY experiment on the 10-mer in H_2O solution a jump–return (JR) observation pulse was used for selective excitation (Guéron et al., 1991) with subsequent post-acqusition solvent suppression (Sodano & Delepierre, 1993). The one-dimensional spectra of the 10-mer in H_2O solution were acquired with the $1\bar{3}3\bar{1}$ pulse for water suppression (Hore, 1983) on the Varian spectrometer, except for the melting experiments which were acquired on a JEOL Alpha 400-MHz spectrometer with a JR pulse. The software package FELIX (Biosym Inc.) was used for NMR data processing. The program MARDIGRAS (obtained from Dr. T. James, University of California, San Francisco, CA; Borgias et al., 1990) was used for estimating proton–proton distances from NOESY data, with the NOE cross-peak intensities, measured by integration, as input data. The similarity between the interproton distances obtained by MARDIGRAS and those in canonical A- or B-form DNA was measured by the correlation coefficient, C, defined as

$$C = \frac{\sum (x_i - \bar{x})(y_i - \bar{y})}{\sqrt{\sum (x_i - \bar{x})^2}\sqrt{\sum (y_i - \bar{y})^2}} \qquad (1)$$

where x_i is a distance calculated from NOE intensities by MARDIGRAS, y_i is the corresponding distance in canonical A- or B-DNA, and $\bar{x}$ and $\bar{y}$ refer to the average value of all distances in the two structures compared, respectively. The programs SPHINX and LINSHA (Widmer & Wüthrich, 1987; obtained from Dr. K. Wüthrich, ETH, Zürich, Switzerland) were used for simulation of the DQF-COSY cross-peak patterns.

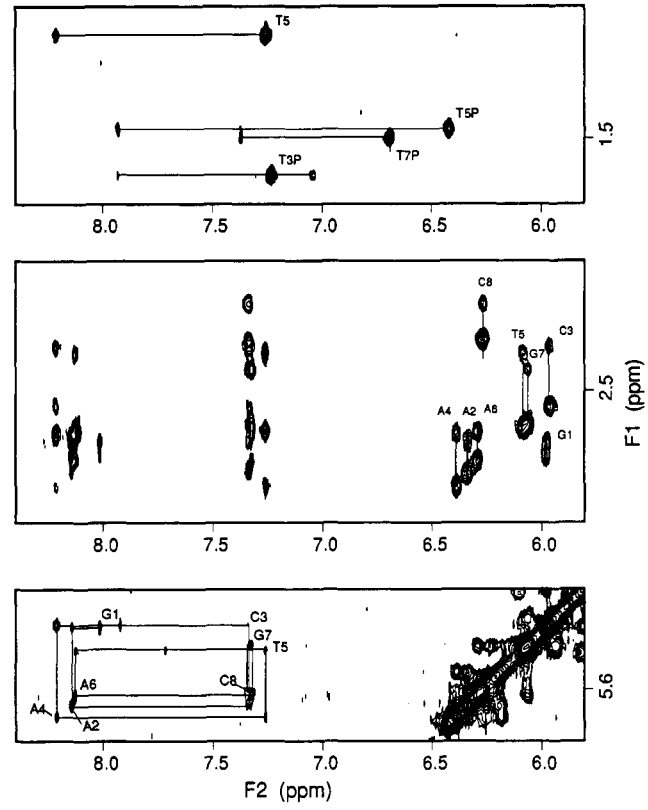

FIGURE 2: NOESY spectrum of the 1:1 complex of the 8-mer PNA–DNA sample (0.6 mM duplex) in D_2O solution at 24 °C and 200-ms mixing time. Panels: aromatic/H1′–methyl region (a, top), aromatic/H1′–H2′/H2″ region (b, middle), and aromatic/H1′–H1′ region with intraresidue assignments indicated (c, bottom).

RESULTS AND DISCUSSION

Two different PNA sequences, one 8-mer and one 10-mer, and their DNA partner strands of antiparallel complementarity (Chart 2) have been studied by ^{1}H NMR.

Chart 2

8-mer: 5′-(G-A-C-A-T-A-G-C)-3′

H_2N-(C-T-G-T-A-T-C-G)-H

10-mer: 5′-(A-G-T-G-A-T-C-T-A-C)-3′

H_2N-(T-C-A-C-T-A-G-A-T-G)-H

One-Dimensional NMR and Duplex Formation. Panels a and b in Figure 1 show the one-dimensional spectra of the PNA and DNA 8-mer single strands, respectively. The PNA strand exhibits a large number of relatively sharp peaks of low intensity, in clear contrast to the DNA strand which gives rise to one sharp resonance per proton. This is evidence that several discrete structural species of the PNA strand are present and that the exchange between these is slow on the NMR time scale. In the ^{1}H NMR spectrum of the PNA 2-mer H-AC-NH_2 four sharp peaks of nonequal intensities are observed for each aromatic proton (data not shown). This demonstrates that a single-stranded 2-mer can adopt four

Table 1: Chemical Shifts, in ppm, of Protons of the 8-mer Duplex at 24 °C (a) and of the 10-mer Duplex at 27 °C (b)

Part a

	H6/H8	H2/H5	H1′	H2′	H2″	H3′	H4′	methyl	imino[a]	amino[a,c]	NH[a]	methylene
G1	8.02		5.98	2.74	2.79	4.83	4.25					
A2	8.14	7.92	6.34	2.74	2.88	4.98	4.46					
C3	7.34	5.13	5.97	2.30	2.57	4.82	4.33			8.28/6.93		
A4	8.21	7.72	6.39	2.70	2.94	4.93	4.50					
T5	7.26		6.09	2.33	2.67	4.91		1.04	13.57			
A6	8.13	6.95	6.29	2.69	2.82	4.98	4.47					
G7	7.32		6.06	2.40	2.65	4.81	4.42		12.98			
C8	7.34	5.13	6.28	2.10	2.26	4.48	4.15			8.28/6.93		
G1P	7.96											
C2P	7.05	5.39								8.38/6.95	8.77	4.22
T3P	7.23							1.67	13.48		8.59	3.91
A4P	7.93	6.96									8.69	3.88
T5P	6.42							1.46	13.51		8.69	3.37
G6P	7.37								12.83		8.53	4.47
T7P	6.70							1.49	14.24		8.78	3.60
C8P	7.28	5.65								8.52/7.21	8.41	3.84

Part b

	H6/H8	H2/H5	H1′	H2′	H2″	H3′	H4′	methyl	imino[b]	amino[b,c]	NH[b]	methylene
A1	8.09		6.15	2.47	2.60							
G2	7.92		5.99	2.70	2.83				13.15			
T3	7.36		6.14	2.38	2.67			1.19	13.89			
G4	7.75		6.06	2.63	2.73				11.64	7.50/6.43		
A5	7.85	7.83	6.35	2.61	2.85					7.88/6.46		
T6	7.29		6.11	2.31	2.59			0.94	13.91			
C7	7.57	5.53	6.11	2.22	2.59					8.17/6.91		
T8	7.57		6.14	2.37	2.67			1.44	13.65			
A9	8.13	6.87	6.27	2.56	2.74					7.62/6.21		
C10	7.24		6.19	2.03	2.17							
G1P	7.51											
T2P	7.00							1.49			8.36	
A3P												
G4P									12.24	8.57/5.87		
A5P	7.22	7.83								7.86/6.68	8.81	
T6P	6.40							1.39	14.24		8.75	
C7P	7.19	5.53								8.22/7.06	8.46	
A8P	7.93	7.41										
C9P	6.61	5.45								8.52/7.22	8.58	
T10P	6.69							1.52			8.52	

[a] Measured at 14 °C. [b] Measured at 8 °C, 50 mM phosphate buffer, pH 7.0. [c] Low-field chemical shift refers to base-pairing proton resonance.

different conformations, presumably two backbone amide bond rotamers per residue, that exchange slowly. In a longer PNA sequence this would result in a multitude of resonances, as observed (Figure 1a). Figure 1c shows the spectrum of the PNA–DNA 8-mer complex at a 1:1 stoichiometric ratio. The number of resonances from the PNA strand is reduced to one per proton, demonstrating that in the duplex only one conformation is present. The chemical shifts of several proton resonances, on the DNA as well as on the PNA strand, change considerably as the two strands are mixed, indicating that structural alterations take place in both strands upon hybridization.

Two-Dimensional NMR and Resonance Assignment. Selected regions of a two-dimensional NOESY spectrum of the 8-mer are shown in Figure 2. The DNA aromatic and sugar protons could be assigned by standard procedures (Hare et al., 1983), as indicated in the aromatic–H1′ region in Figure 2c (the assignments are listed in Table 1). The protons on the DNA strand exhibit some chemical shift differences in comparison with what is normally observed for DNA–DNA duplexes (Majmudar & Hosur, 1992). For example, the sugar H1′ resonances appear within a relatively narrow range that is shifted downfield by a few tenths of a ppm, whereas the methyl resonances are shifted slightly upfield.

The assignment of the PNA strand protons was less straightforward since no continuous sequentially connecting cross-peak pattern could be used. The aromatic protons of the PNA thymines and their flanking base(s) were identified by their cross-peaks with the methyl protons (as indicated in Figure 2a). Similarly, the H5–H6 proton cross-peaks were used to identify the cytosine bases. The imino protons, assigned from their interactions with the DNA strand, were useful for confirming the sequential assignments and for assigning the other exchangeable protons. A few comments may be made regarding the chemical shifts of the PNA protons (cf. Table 1). The aromatic PNA protons are generally shifted upfield, as compared to a DNA–DNA duplex. This is particularly pronounced for the H6 protons of the thymines, which can be found as far upfield as 6.4 ppm. The amide protons in the PNA backbone appear between 8.4 and 8.9 ppm. These protons were assigned from their NOE cross-peaks to the aromatic protons on the same residue and from their weaker NOEs to the aromatic protons on the flanking residue on the N-terminal side. In addition, a few weak sequential amide–amide cross-peaks were seen, supporting the assignments. The methylene proton resonances appear around 3.4–4.5 ppm (with the exception of the isolated pair of methylene protons located between the tertiary nitrogen and the carboxy group on the backbone, which we tentatively have assigned to the 5.8–6.5 ppm region). However, complete assignments of the PNA protons have not been accomplished at this stage, partly due to extensive overlaps among the methylene protons. Moreover, the low solubility of the PNA–DNA duplex (~1 mM) limits

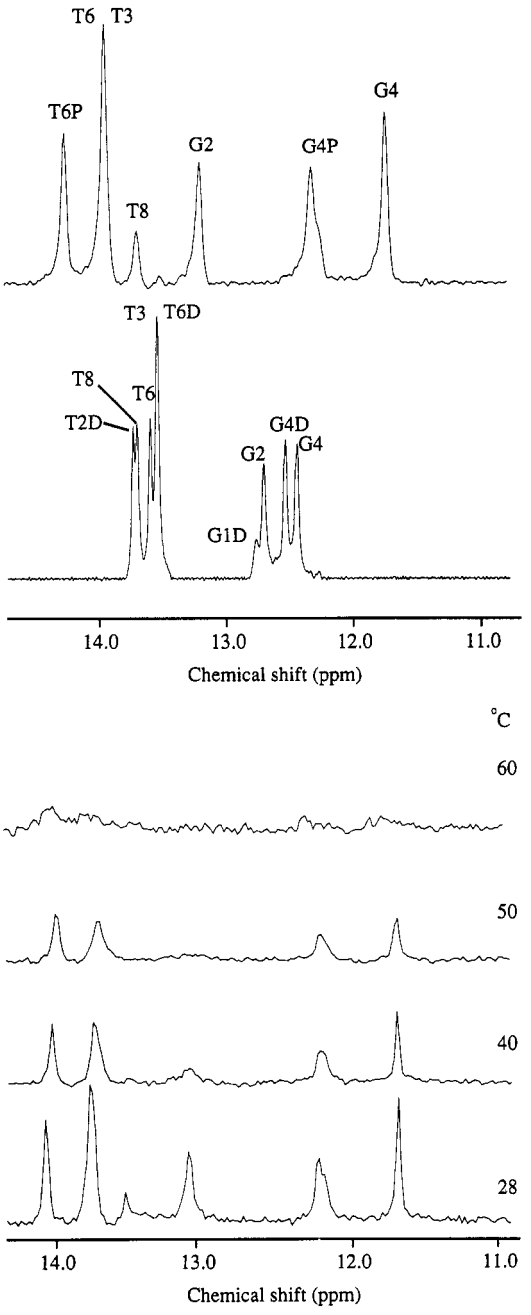

FIGURE 3: (a, top panel) ^{1}H NMR spectra of the imino proton region of the 10-mer PNA–DNA complex at a 1:1 ratio (top spectrum) and of the corresponding DNA–DNA complex (bottom spectrum) at 8 °C. P refers to protons on the PNA strand and D to protons on the DNA strand with the same sequence as the PNA strand. (b, bottom panel) Imino region of the same PNA–DNA complex at different temperatures.

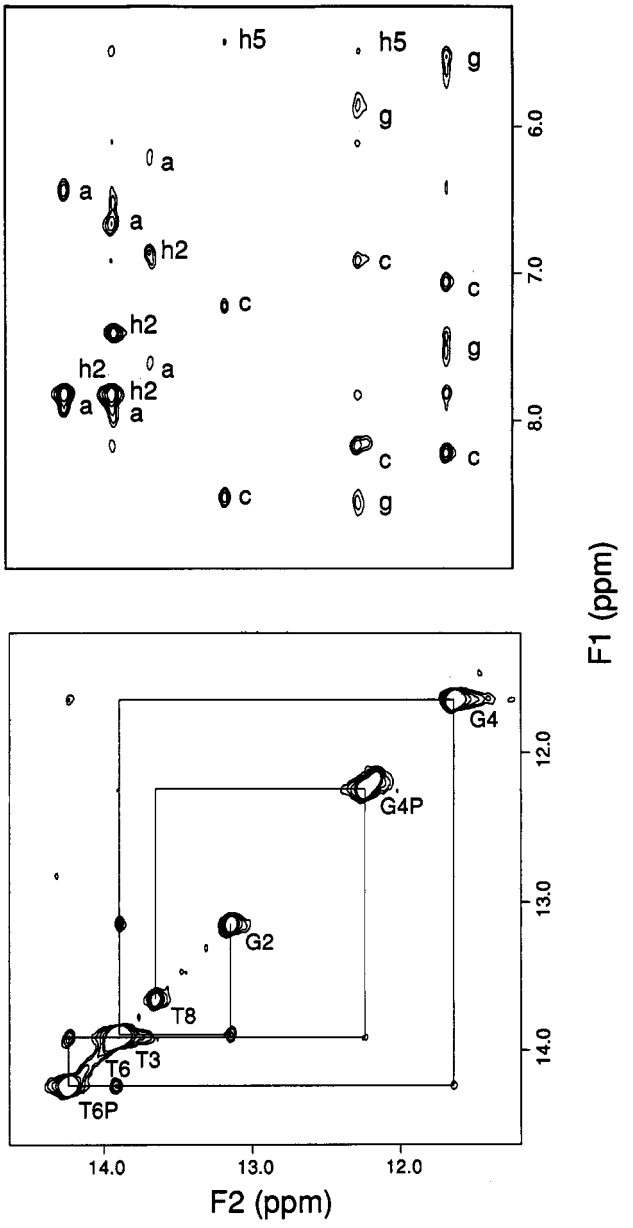

FIGURE 4: NOESY spectrum of the 10-mer PNA–DNA duplex (0.9 mM duplex) in H_2O solution at 8 °C and 250-ms mixing time. Panels: imino–aromatic/amino region with adenine H2, cytosine H5, and adenine, cytosine, and guanine amino proton cross-peaks indicated as h2, h5, a, c, and g, respectively (a, top), and imino–imino region with sequential assignments indicated (b, bottom).

the cross-peak intensities and thereby makes assignment difficult.

Imino Protons and Base Pairing. The imino proton region of the one-dimensional spectra of the PNA–DNA 10-mer complex and its corresponding DNA–DNA duplex is shown in Figure 3a. In both complexes seven imino proton resonances are observed, i.e., one per base pair with the exception of the less stable end base pairs. It is interesting to note that the dispersion of the chemical shifts is larger in the PNA–DNA complex than in the DNA–DNA duplex, indicating that the base-pair stacking is less regular in the PNA–DNA hybrid. The fact that the imino protons give rise to resonances that are relatively sharp and intense suggests that they are stabilized by hydrogen bonds, presumably by being engaged in base pairing. The temperature dependence of the imino proton resonances is shown in Figure 3b. It is seen that the melting of the PNA–DNA complex occurs between 50 and 60 °C, which may be compared to the optically determined melting temperatures of 48 and 40 °C for the antiparallel and parallel duplexes, respectively. It can also be concluded that the strand separation propagates from the ends of the duplex. In addition, it should be mentioned here that the optically measured melting temperatures of the PNA–DNA 8-mer were 30 and 31 °C in the antiparallel and parallel complexes, respectively.

The NOESY spectrum of the PNA–DNA 10-mer duplex in H_2O solution at 8 °C exhibits several cross-peaks involving imino protons, shown in Figure 4. Sequential cross-peaks between the imino protons indicate base-pair stacking along the sequence (Figure 4b). In the imino–aromatic/amino proton region (Figure 4a) strong cross-peaks are seen between the thymine imino and adenine H2 protons within the AT base pairs. In the GC base pairs, relatively strong cross-

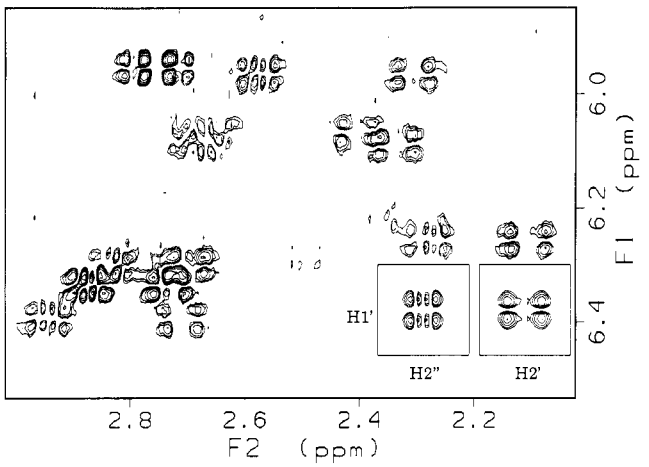

FIGURE 5: DQF-COSY of the PNA–DNA 8-mer duplex (1.1 mM duplex) in D_2O at 24 °C at the H2′/H2″–H1′ region. Inserts show simulated H1′–H2′ and H1′–H2″ cross-peaks, assuming rapid interconversion between the C2′-*endo* and C3′-*endo* conformations (96% in the C2′-*endo*). The coupling constants used were $J_{1'2'}$ = 9.0 Hz, $J_{1'2''}$ = 6.5 Hz, $J_{2'2''}$ = −14.0 Hz, $J_{2'3'}$ = 7.8 Hz, and $J_{2''3'}$ = 0.5 Hz.

peaks between the guanine imino protons and the amino protons on the pairing cytosine are seen (indicated c in Figure 4a). These observations demonstrate short interproton distances and hydrogen bonds that strongly argue for Watson–Crick base pairing. Furthermore, the amino proton resonances of all the bases are visible at this temperature, demonstrating slow rotation of the amino groups, consistent with their participation in the base pairing. We also note that no strong cross-peaks are observed between imino protons and the H6/H8 or H5 protons on the partner base, in agreement with Watson–Crick-type base pairing and excluding Hoogsteen base pairing.

Quantitative Measurements and Structural Correlation. The cross-peak pattern seen in the NOESY spectra strongly indicates that the DNA strand is in a B-like conformation. First, in the aromatic–H1′ region the inter- and intraresidue cross-peaks are of comparable intensities (Figure 2c). Second, in the aromatic–H2′/H2″ region the aromatic protons show stronger intraresidual cross-peaks with the H2′ than with the H2″ protons (Figure 2b). Third, the intraresidue cross-peaks between the aromatic and the H3′ protons are very weak (data not shown), which is also in support of the sugar puckers being in the C2′-*endo* range. These observations suggest that the glycosidic torsion angles preferably adopt the *anti* conformation and that the sugar puckers are close to C2′-*endo*, consistent with a B-like conformation (Wüthrich, 1986). The similar intensities of the intra- and interresidue cross-peaks in the aromatic–H1′ region also show that there are no extreme irregularities in the base stacking of the DNA strand. However, unusually strong sequential cross-peaks are observed between the adenine H2 protons, located in the minor groove, and the H1′ protons on the 3′-flanking sugar, indicating a compressed minor groove (Chen et al., 1992).

Additional evidence that a B-like conformation is favored by the DNA sugars is provided by a DQF-COSY spectrum (Figure 5). The cross-peaks in the H2′/H2″–H1′ region exhibit C2′-*endo* splitting patterns (Rinkel & Altona, 1987; Schmitz et al., 1990), which can be seen from comparison with cross-peaks simulated from coupling constants typical of the C2′-*endo* conformation (insert in Figure 5). From this, and in consistency with the NOESY data, we conclude that each DNA residue predominantly (>80%) resides in the C2′-*endo* conformation, typical for B-DNA.

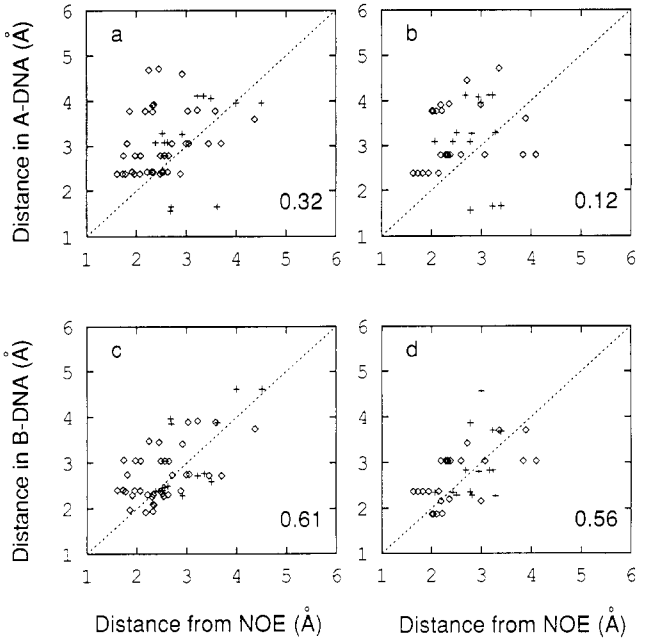

FIGURE 6: Correlation between proton–proton distances in the DNA strand of the 1:1 PNA–DNA complexes derived from NOESY cross-peak intensities using MARDIGRAS with canonical B-DNA as the starting structure and distances in canonical A- and B-form DNA for the 8-mer (a and c) and for the 10-mer (b and d). Intraresidue distances (◇), sequential distances (+), and correlation coefficients, given by eq 1, are shown.

Preliminary analyses of the overall structures of the DNA strands in the two PNA–DNA duplexes were performed. Interproton distances were estimated from NOESY cross-peak intensities, and modeling was done with the program MARDIGRAS, which allows full relaxation matrix treatment of the data (Borgias et al., 1990). NOESY data of the 8-mer and the 10-mer, collected with mixing times of 200 and 150 ms, respectively, were used, and canonical A- and B-form DNAs were taken as starting structures. The number of interproton distances used for the 8-mer and the 10-mer was 40 and 23 intraresidual and 13 and 14 sequential, respectively. The distances starting from the A- and B-conformations converged closely, with correlation coefficients, C (eq 1), of 0.9 for the 8-mer and 0.8 for the 10-mer (C = 1 corresponds to identity). The resulting distances were then compared to the corresponding distances in canonical A- and B-DNA, as shown in Figure 6. For both the 8-mer and the 10-mer, the data show a closer resemblance with B-DNA. Since the structure modeling was based on more intra- than interresidue NOE cross-peaks, the accuracy of the structure within each residue is relatively high, whereas the position of one residue relative to its neighbor is less well determined. Therefore, it seems possible that the stacking of the DNA bases may differ somewhat from B-form DNA. Minor differences in the base-pair stacking would also be consistent with the larger dispersion of the chemical shifts observed for both the aromatic and the imino protons of the PNA–DNA hybrids. Furthermore, the CD spectrum of the 8-mer PNA–DNA duplex provides support for the structure being a right-handed helix (results not shown).

CONCLUSIONS

The results presented here show that PNA–DNA duplexes can be kept at concentrations that allow ^{1}H-NMR studies to be conducted and that the structural stability of the PNA strand, induced by the DNA strand, makes such studies feasible. The resonances of the DNA strand protons can easily be assigned by the same approach as in a regular B-form

DNA duplex, and their chemical shifts are, with a few minor exceptions, similar to those found in DNA duplexes. The PNA protons were most successfully assigned from the H_2O data, since the base-pairing imino protons, as well as the backbone amide protons, were very useful in the assignment procedure. The chemical shifts of the PNA base protons were found to deviate somewhat from the corresponding type of protons on the DNA strand, generally shifting upfield, thus reducing the problem of overlapping resonances. From the NOESY cross-peaks observed it is concluded that duplex formation occurs via hydrogen bonds of Watson–Crick type. It is also concluded that the PNA–DNA duplex is a right-handed helix. Furthermore, preliminary quantitative interpretations of the NOESY data show that the DNA strand is more similar to B-DNA than to A-DNA. In agreement with this, the COSY data demonstrate that the deoxyribose sugars of the DNA strand adopt the C2′-*endo* conformation typical of B-form DNA. The data presented here provide the first conclusive evidence regarding the structure and conformation of a PNA–DNA duplex. However, more complete assignments of the PNA proton resonances are necessary before a refined structure of the whole duplex can be determined (work in progress). The PNA–DNA duplex study can also be regarded as a necessary step before undertaking NMR studies of $(PNA)_2DNA$ triplexes or PNA–PNA duplexes.

ACKNOWLEDGMENT

We thank Dr. M. Sarkar and Mr. S. Tomac of Stockholm University and Mrs. A. W. Jørgensen of the H. C. Ø. Institute, Copenhagen, for optical studies of melting temperatures and Mr. J. Zdunek of the University of Umeå for helpful discussions. We also thank the Swedish NMR Center and the Protein NMR Center, Department of Chemistry, University of Copenhagen, for access to their 500-MHz spectrometers.

REFERENCES

Boelens, R., Scheek, R. M., Dijkstra, K., & Kaptein, R. (1985) *J. Magn. Reson. 62,* 378–386.

Borgias, B. A., Dochin, M., Kerwood, D. J., & James, T. L. (1990) *Prog. Nucl. Magn. Reson. Spectrosc. 22,* 83–100.

Chen, S., Leupin, W., & Chazin, W. J. (1992) *Int. J. Biol. Macromol. 14,* 57–63.

Cherny, D. Y., Belotserkovskii, B. P., Frank-Kamenetskii, M. D., Egholm, M., Buchardt, O., Berg, R. H., & Nielsen, P. E. (1993) *Proc. Natl. Acad. Sci. U.S.A. 90,* 1667–1670.

Demidov, V., Frank-Kamenetskii, M. D., Egholm, M., Buchardt, O., & Nielsen, P. E. (1993) *Nucleic Acids Res. 21,* 2103–2107.

Demidov, V., Potaman, V. N., Frank-Kamenetskii, M. D., Egholm, M., & Nielsen, P. E. (1994) *Biochem. Pharmacol.* (in press).

Egholm, M., Buchardt, O., Nielsen, P. E., & Berg, R. H. (1992) *J. Am. Chem. Soc. 114,* 1895–1897.

Egholm, M., Buchardt, O., Christensen, L., Behrens, C., Freier, S. M., Driver, D. A., Berg, R. H., Kim, S. K., Nordén, B., & Nielsen, P. E. (1993) *Nature 365,* 566–568.

Guéron, M., Plateau, P., & Decorps, M. (1991) *Prog. Nucl. Magn. Reson. Spectrosc. 23,* 135–219.

Hanvey, J. C., Peffer, N. J., Bisi, J. E., Thomson, S. A., Cadilla, R., Josey, J. A., Ricca, D. J., Hassman, C. F., Bonham, M. A., Au, K. G., Carter, S. G., Bruckstein, D. A., Boyd, A. L., Noble, S. A., & Babiss, L. E. (1992) *Science 258,* 1481–1485.

Hare, D. R., Wemmer, D. E., Chou, S.-H., Drobny, G., & Reid, B. (1983) *J. Mol. Biol. 171,* 319–336.

Hore, P. J. (1983) *J. Magn. Reson. 55,* 283–300.

Kim, S. K., Nielsen, P. E., Egholm, M., Buchardt, O., Berg, R. H., & Nordén, B. (1993) *J. Am. Chem. Soc. 115,* 6477–6481

Majmudar, A., & Hosur, R. V. (1992) *Prog. Nucl. Magn. Reson. Spectrosc. 24,* 109–158.

Marion, D., & Wüthrich, K. (1983) *Biochem. Biophys. Res. Commun. 113,* 967–974.

Nielsen, P. E., Egholm, M., Berg, R. H., & Buchardt, O. (1991) *Science 254,* 1497–1500.

Ørum, H., Nielsen, P. E., Egholm, M., Berg, R. H., Buchardt, O., & Stanley, C. (1993) *Nucleic Acids Res. 21,* 5332–5336.

Rinkel, L., & Altona, C. (1987) *J. Biomol. Struct. Dyn. 4,* 621–649.

Schmitz, U., Zon, G., & James, T. L. (1990) *Biochemistry 29,* 2357–2368.

Sodano, P., & Delepierre, M. (1993) *J. Magn. Reson. 104,* 88–92.

States, D. J., Haberkorn, R. A., & Ruben, D. J. (1982) *J. Magn. Reson. 48,* 286–292.

Widmer, H., & Wüthrich, K. (1987) *J. Magn. Reson. 74,* 316–336.

Wittung, P., Nielsen, P. E., Buchardt, O., Egholm, M., & Nordén, B. (1994) *Nature 368,* 561–563.

Wüthrich, K. (1986) *NMR of Proteins and Nucleic Acids,* Wiley, New York.